

Nano Ag-enhanced energy conversion efficiency in standard commercial pc-Si solar cells and numerical simulations with finite difference time domain method

Jing Yu, Weijia Shao, Yao Zhou, Huijie Wang, Xiao Liu, and Xiaoliang Xu

Citation: [Applied Physics Letters](#) **103**, 203904 (2013); doi: 10.1063/1.4830418

View online: <http://dx.doi.org/10.1063/1.4830418>

View Table of Contents: <http://scitation.aip.org/content/aip/journal/apl/103/20?ver=pdfcov>

Published by the [AIP Publishing](#)

Articles you may be interested in

[Enhancement of short-circuit current density in polymer bulk heterojunction solar cells comprising plasmonic silver nanowires](#)

Appl. Phys. Lett. **104**, 123302 (2014); 10.1063/1.4869760

[Boosting Cu₂ZnSnS₄ solar cells efficiency by a thin Ag intermediate layer between absorber and back contact](#)

Appl. Phys. Lett. **104**, 041115 (2014); 10.1063/1.4863951

[Efficiency enhancement of polymer solar cells by localized surface plasmon of Au nanoparticles](#)

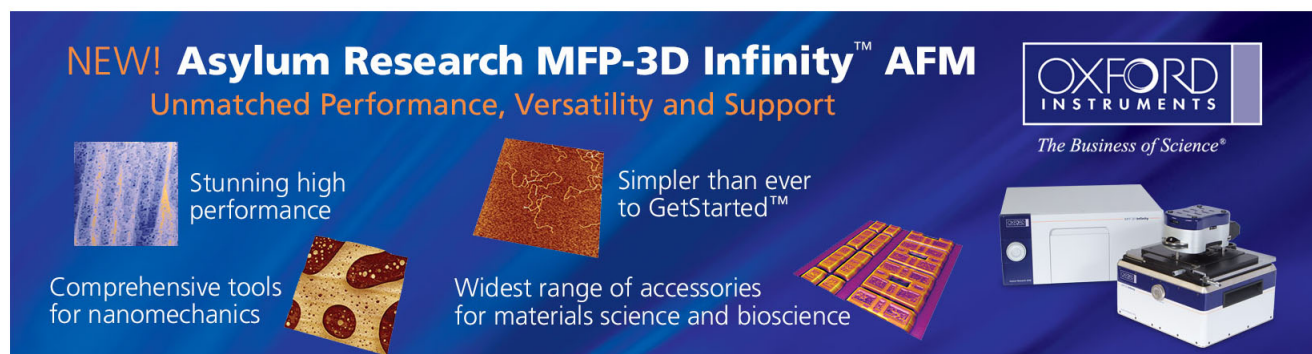
J. Appl. Phys. **114**, 163102 (2013); 10.1063/1.4827181

[Nano-particle based scattering layers for optical efficiency enhancement of organic light-emitting diodes and organic solar cells](#)

J. Appl. Phys. **113**, 204502 (2013); 10.1063/1.4807000

[The role of Ag nanoparticles in inverted polymer solar cells: Surface plasmon resonance and backscattering centers](#)

Appl. Phys. Lett. **102**, 123301 (2013); 10.1063/1.4798553



NEW! Asylum Research MFP-3D Infinity™ AFM
Unmatched Performance, Versatility and Support

OXFORD INSTRUMENTS
The Business of Science®

Stunning high performance
Simpler than ever to GetStarted™
Comprehensive tools for nanomechanics
Widest range of accessories for materials science and bioscience

The advertisement features several images: a blue textured surface, a brown textured surface, a grid of colorful rectangular samples, and the Asylum Research MFP-3D Infinity AFM instrument.

Nano Ag-enhanced energy conversion efficiency in standard commercial pc-Si solar cells and numerical simulations with finite difference time domain method

Jing Yu (郁菁), Weijia Shao (邵伟佳), Yao Zhou (周尧), Huijie Wang (王会杰),
 Xiao Liu (刘骁), and Xiaoliang Xu (许小亮)^{a)}

Department of Physics, University of Science and Technology of China, Hefei, Anhui 230026, China

(Received 29 June 2013; accepted 21 October 2013; published online 15 November 2013)

Nano Ag-enhanced energy conversion efficiency (*ECE*) in one standard commercial pc-Si solar cell utilizing the forward scattering by Ag nanoparticles on surface has been researched experimentally and simulatively in this paper. Directly assembling Ag nanoparticles (with size about 100 nm) on the surface, it is found when the particle surface coverage is 10%, the *ECE* and the short circuit current density are increased by 2.8% and 1.4%, respectively. Without changing any existing structure of the ready-made solar cell, this facile and efficient method has huger applications than other methods. © 2013 AIP Publishing LLC. [<http://dx.doi.org/10.1063/1.4830418>]

Crystalline silicon solar cells always occupy the dominant position in photovoltaic market during the past decade, therein poly-crystalline silicon (pc-Si) solar cell is the most popular and wide-used product due to its low cost in contrast with single-crystalline silicon (sc-Si) solar cell and high energy conversion efficiency (*ECE*) compared with amorphous silicon (a-Si) solar cell.^{1,2} Surface texturing (ST) and antireflection coating (ARC) are the common methods used in producing pc-Si solar cell, which can significantly increase the effective absorption of the incident lights.¹⁻³ Nevertheless, the *ECE* of pc-Si solar cell is still lower than that of sc-Si solar cell, which impels researchers realize the importance of exploring new methods to further improve the lights absorption of pc-Si solar cell. A promising way to achieve this goal is taking use of the forward scattering of the plasmonic effect excited by metal nanoparticles (Au, Ag, Al, etc.),⁴⁻¹¹ where Ag nanoparticles are widely used due to its relative low price in contrast with Au and well controllability in synthesis compared with Al.^{5,9,12-14} Incident lights will scatter preferentially into the larger-permittivity dielectric when Ag nanoparticles are put on the interface between two dielectrics, resulting in an angular spread which can induce an increase of optical path length.^{4,15} Based on this principle, various Ag-enhanced Si solar cells have been studied by researchers, including thin sc-Si solar cell, bulk sc-Si solar cell, thin a-Si solar cell, and thin pc-Si solar cell.^{5,16-20} But, most of the above solar cells are planar structures with or without ARC, where ST is often ignored. Taking Ag as a scattering particles and combining with ARC and ST all together will adequately utilize these three light-trapping effects and consequently increase the *ECE* of Si solar cells, Fahr's group²¹ had reported a similar structure in tandem Si solar cells which showed a great enhancement of current densities from 11.67 mA/cm² to 14.48 mA/cm². However, there is little relevant research on pc-Si solar cell. What is more, although all the researches above show great *ECE* enhancements in various Si solar cells, they are far

from practical application due to their complex preparation procedures and large alterations in existing structures of Si solar cell. Studies in ready-made commercial pc-Si solar cells are barely researched, making the practical application of Ag-enhanced Si solar cells in daily life still no obvious breakthrough.

In this paper, Ag nanoparticles are placed randomly on the surface of one commercial pc-Si solar cell (2 cm × 2 cm × 180 μm, Suiying Solar Technology Co., Shanghai, China), which is excellently textured and coated with about 75 nm SiN_x ARC. Three surface coverages (SC) (5%, 10%, and 20%) of Ag nanoparticles were tried in our test, and different increases of *ECE* and short circuit current density (*J_{sc}*) were observed. When the SC was 10% and the size of Ag nanoparticles was about 100 nm, best result was obtained: *J_{sc}* increased from 32.00 mA/cm² to 32.45 mA/cm² and *ECE* increased from 14.00% to 14.39%, which were enhanced by 1.4% and 2.8%, respectively. The present manufacture technology of commercial pc-Si solar cell is full-fledged, the *ECE* is steady and harder to increase, so this improvement is undoubtedly very exciting. Because the enhancements are obtained on ready-made commercial pc-Si solar cells which are widely available in markets, this simple process has huger applications compared with other methods. Relevant numerical simulations by finite difference time domain (FDTD) method, which provide a good understanding of the experimental results, are also presented in this paper. Figure 1 shows the schematic of forward scattering by Ag nanoparticles on the surfaces of the commercial pc-Si solar cells.

Ag nanoparticles were synthesized by a modified method reported by Silvert *et al.*,²² where 0.05 g silver nitrate (AgNO₃, 99.8%, AR), 0.18 g polyvinylpyrrolidone (PVP, *M_w* = 55 000), and 20 ml ethylene glycol (C₂H₆O₂, 99.0%, AR) were mixed uniformly and heated at 130 °C for 1 h. Then these Ag nanoparticles were washed with absolute ethyl alcohol (EtOH, 95%, AR) for several times and dispersed in the EtOH for further use. The nanoparticles synthesized by this method were size-consistent with particle diameter about 100 nm. The inset in Figure 2(b) is the transmission electron microscope (TEM, JEM-2011) image of the Ag nanoparticles.

^{a)} Author to whom correspondence should be addressed. Electronic mail: xlxu@ustc.edu.cn

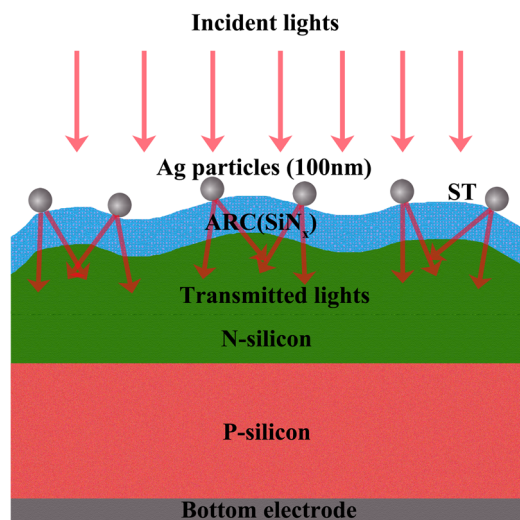


FIG. 1. Schematic of forward scattering by Ag nanoparticles on the surface of the commercial pc-Si solar cell.

The solution of Ag nanoparticles was dropped on the surface of pc-Si solar cell directly, after the EtOH evaporating thoroughly the solution was dropped again, then same process was repeated several times. By controlling the drop times, surfaces with three SC (5%, 10%, and 20%) of Ag nanoparticles were obtained. Figure 2 is the scanning electron microscope (SEM, JSM-6700F) images of the surfaces with different Ag SC: (a) no Ag, (b) SC = 5%, (c) SC = 10%, and (d) SC = 20%.

Current density-voltage (J - V) and power-voltage (P - V) characterizations of the pc-Si solar cells with different Ag SC were tested by the solar simulator (OTENTO-SUN II, Bunkoukeiki. co. Ltd.), and J_{sc} , open circuit voltage (V_{oc}), ECE and fill factor (FF) are all shown in Table I.

Figure 3 indicates that the maximum power (MP) of the commercial pc-Si solar cell without any Ag nanoparticles on

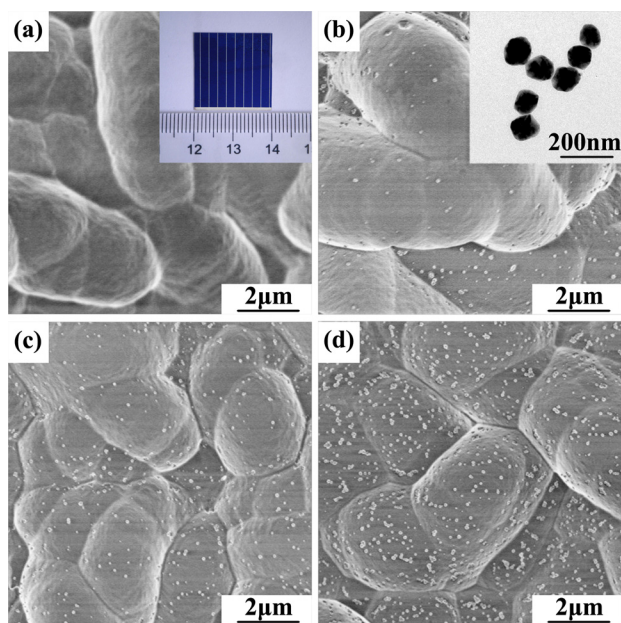


FIG. 2. SEM images of commercial pc-Si solar cells with different Ag SC: (a) SC = 0%, (b) SC = 5%, (c) SC = 10%, (d) SC = 20%, inset in (a) the photograph of the commercial pc-Si solar cell, inset in (b) the TEM image of the Ag nanoparticles.

TABLE I. Short circuit current density, open circuit voltage, energy conversion efficiency, and fill factor with different Ag SC.

	No Ag	SC = 5%	SC = 10%	SC = 20%
J_{sc} (mA/cm ²)	32.00	32.12	32.45	31.94
V_{oc} (V)	0.591	0.590	0.592	0.589
ECE (%)	14.00	14.06	14.39	13.88
FF	0.740	0.742	0.749	0.738

its surface is 14.00 mW/cm², and when SC = 5% and 10% the MP increases to 14.06 mW/cm² and 14.39 mW/cm², respectively, but when SC = 20% the MP decreases to 13.88 mW/cm². The same variation tendencies of J_{sc} , ECE and FF are also observed in Table I, where the three parameters are increased by 1.4%, 2.8%, and 1.2%, respectively, in contrast with the primal pc-Si solar cell when the SC = 10%. These enhancements are mainly due to the forward scattering of Ag nanoparticles, which effectively increases the optical path length of the incident lights then improves the lights absorption combining with the ST and ARC together and finally turns into excess photo-generated carriers. For low SC (5%) the improvement is not so obvious, because there are not sufficient Ag nanoparticles to provide adequate lights absorption. But, for high SC (20%), too many Ag nanoparticles on the surfaces will hinder the lights to enter into the pc-Si and decrease the absorption of the incident lights.

For better understanding the forward scattering effect and experimental results above, the transmittance, electric field distribution, and absorption profiles of pc-Si solar cells were simulated, using the software FDTD Solutions,²³ where planar pc-Si solar cells with 75 nm Si₃N₄ ARC and different Ag SC were adopted. As shown in Figure 4(a), perfectly matched layer boundary conditions were used in z-direction and periodic boundary conditions were used in x/y-direction. Setting the diameter of Ag nanoparticles to 100 nm and different SC can be obtained by changing the intervals between two particles.

Figure 4(b) shows the simulated transmittance of the planar pc-Si solar cells ($T_{sim}(\lambda)$) with different Ag SC. When Ag nanoparticles are put on the surfaces of the solar cells, the transmittance enhancement and suppression occurs at wavelength above and below 680 nm (SC = 10%, different SC slightly shifts), respectively. As we inferred previously, we consider that these enhancements come from the forward scattering effect of Ag nanoparticles. Figures 5(a) and 5(b)

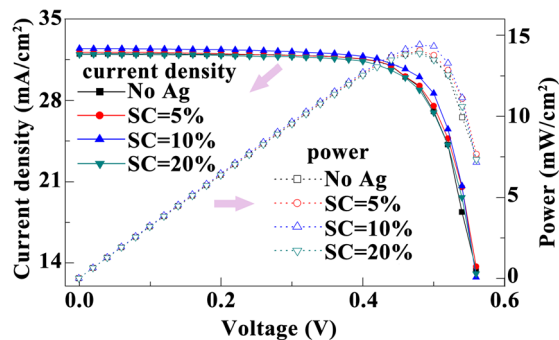


FIG. 3. Current density-voltage (J - V) and power-voltage (P - V) characterizations of commercial pc-Si solar cells with different Ag SC.

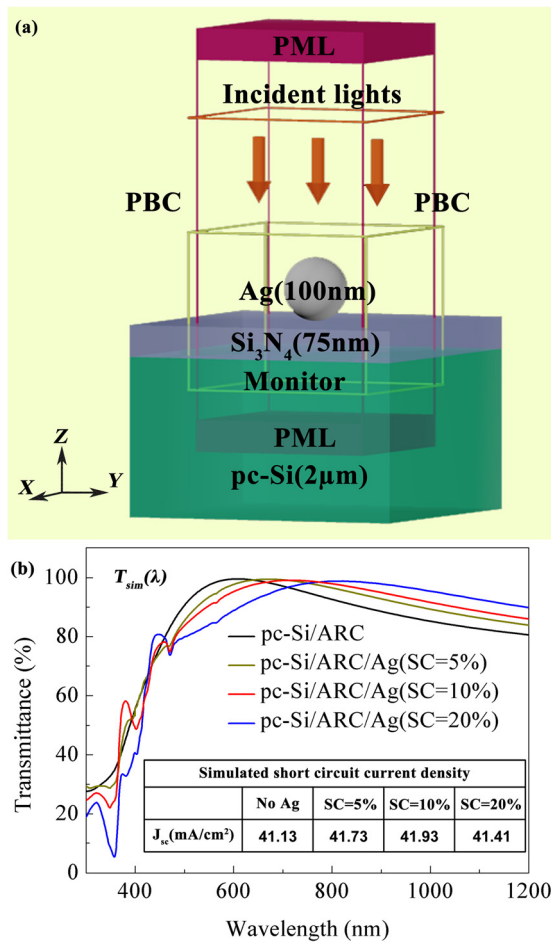


FIG. 4. (a) Schematic of the simulation model used in FDTD solutions, (b) simulated transmittance of the planar pc-Si solar cells with different Ag SC.

show the simulated electric field distribution ($\lambda = 729$ nm) of pc-Si/ARC and pc-Si/ARC/Ag (SC = 10%) in x-y plane below Si_3N_4 ARC 5 nm, respectively. Transmitted electric field intensity of the pc-Si/ARC/Ag (SC = 10%) is obviously improved in contrast with that of pc-Si/ARC, which is coincident with $T_{sim}(\lambda)$ above, vividly suggesting Ag nanoparticles can indeed result in certain lights streaming into pc-Si more facile. On account of the position of the transmitted electric field intensity (80 nm below the surface), this improvement cannot come from the near-field enhancement of the localized surface plasmon by Ag nanoparticles, and the only reason for it is the far-field scattering effect (forward scattering effect). For further researching the light absorption by pc-Si, power absorption per unit volume ($L(\vec{r}, \lambda)$) was calculated by

$$\begin{aligned}
 L(\vec{r}, \lambda) &= \frac{1}{2} \text{real} \nabla \cdot (\vec{E}(\vec{r}, \lambda) \times \vec{H}(\vec{r}, \lambda)) \\
 &= \frac{1}{2} \omega |\vec{E}(\vec{r}, \lambda)|^2 \text{Im}(\epsilon_{pc-Si}(\lambda)).
 \end{aligned} \quad (1)$$

Figures 5(c)–5(f) are the simulated absorption profiles of pc-Si/ARC and pc-Si/ARC/Ag (SC = 10%) at $\lambda = 729$ nm, where (c) and (d) are in x-y plane below the Si_3N_4 ARC 5 nm, and (e) and (f) are in y-z plane at $x = 0$. Figures 5(c) and 5(d) are fundamentally the same as Figures 5(a) and 5(b), respectively, indicating that the transmitted light can be well

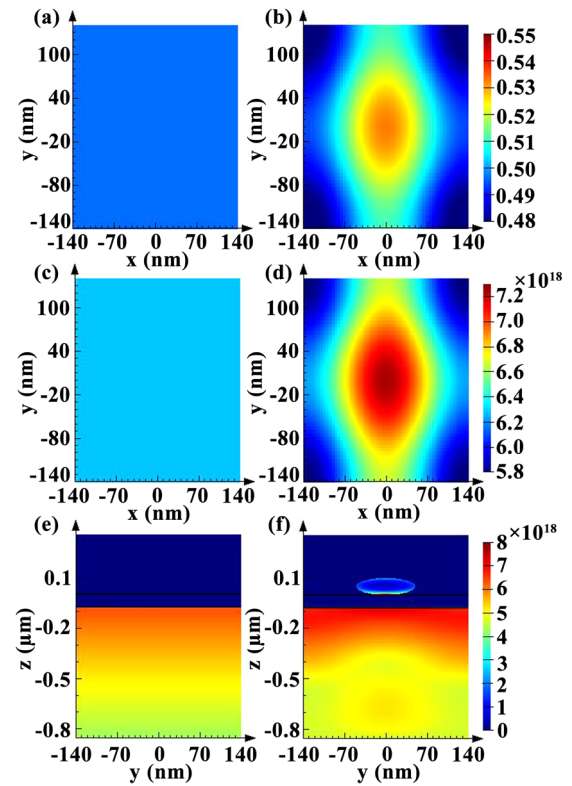


FIG. 5. (a), (b) Simulated electric field distribution ($\lambda = 729$ nm) in x-y plane below Si_3N_4 ARC 5 nm; (c), (d) simulated absorption profiles ($\lambda = 729$ nm) in x-y plane below Si_3N_4 ARC 5 nm; (e), (f) simulated absorption profiles ($\lambda = 729$ nm) in y-z plane ($x = 0$). (a), (c), (e) pc-Si/ARC, (b), (d), (f) pc-Si/ARC/Ag (SC = 10%).

absorbed, in other words suggest that the absorption enhancement (subsequently converting into J_{sc}/ECE enhancement) indeed drives from the forward scattering effect if what we inferred is right. Three areas are divided in Figures 5(e) and 5(f): (1) $z > 0$ nm, air; (2) -75 nm $< z < 0$ nm, Si_3N_4 ; (3) $z < -75$ nm, pc-Si. In areas of air and Si_3N_4 , there are nearly no absorptions due to their ignorable imaginary parts of refractive index, but in the area $z < -75$ nm, absorption is remarkable. In the region -800 nm $< z < -75$ nm, light absorption of pc-Si/ARC/Ag (SC = 10%) is obviously enhanced in contrast with pc-Si/ARC. Compared with Figures 5(a) and 5(b), 5(e) and 5(f) are more convincing in exhibiting the forward scattering effect. It is noticed that the absorption pattern of pc-Si/ARC/Ag (SC = 10%) shows an obvious angular distribution in contrast with that of pc-Si/ARC, which is one characteristic of the forward scattering effect just as we mentioned in the introduction previously. Therefore, combining with the results of (a) and (b), it is reasonable to believe that the enhancement is caused by the forward scattering of Ag nanoparticles. Here $\lambda = 729$ nm was chosen on consideration of its higher transmittance compared with other lights above 680 nm, which can better show the differences of electric field distribution and absorption profiles between pc-Si/ARC and pc-Si/ARC/Ag (SC = 10%). What is more, the transmittance suppression below 680 nm is caused by the Fabry-Perot oscillation, which slightly shifts to longer wavelength when nanoparticles are deposited.

Assuming that all electron-hole pairs contribute to photocurrent, the J_{sc} can be calculated by

$$J_{sc} = e \int \frac{\lambda}{hc} QE(\lambda) I_{AM1.5}(\lambda) d\lambda, \quad (2)$$

where e is the electron charge, h is Planck's constant, c is the speed of light in the free space, λ is the wavelength, $QE(\lambda)$ is the quantum efficiency at the wavelength λ and $I_{AM1.5}(\lambda)$ is the solar spectrum intensity (Air Mass 1.5). $QE(\lambda)$ is defined by

$$QE(\lambda) = \frac{P_{abs}(\lambda)}{P_{in}(\lambda)}, \quad (3)$$

where $P_{in}(\lambda)$ and $P_{abs}(\lambda)$ is the power of the incident light and absorbed light within the solar cell. Because the actual thickness of the pc-Si solar cell is about $180 \mu\text{m}$, sufficient for all lights into pc-Si being absorbed, Eq. (3) is equal to $T_{sim}(\lambda)$. The simulated J_{sc} is shown in the table inserted in Figure 4(b). Comparing with the experimental results, simulations give the same variation tendency of the J_{sc} . When Ag SC = 10%, J_{sc} increase from 41.13 mA/cm^2 to 41.93 mA/cm^2 in contrast with that without Ag covered, which is slightly higher than the experimental result (0.45 mA/cm^2). After all, the simulations are perfectly ideal, and in view of various losses in our practical situation this 0.8 mA/cm^2 increase is acceptable.

In conclusion, Ag-enhanced ECE in standard commercial pc-Si solar cells was researched by us both on experiments and numerical simulations. By dropping Ag solutions on surfaces of commercial pc-Si solar cells, the best result was obtained when Ag SC = 10% with an increase of ECE by 2.8%. On consideration of the handleability of this technique, our experiment provides a useful method for photovoltaic industry.

At last, we sincerely thank the National Natural Science Foundation of China (Grant No. 51272246) and Scientific

and Technological Research Foundation of Anhui (Grant No. 12010202035) for financial support.

- ¹A. Goetzberger, C. Hebling, and H. W. Schock, *Mater. Sci. Eng. R.* **40**, 1 (2003).
- ²J. Zhao, A. Wang, M. A. Green, and F. Ferrazza, *Appl. Phys. Lett.* **73**, 1991 (1998).
- ³P. Panek, M. Lipinski, and J. Dutkiewicz, *J. Mater. Sci.* **40**, 1459 (2005).
- ⁴H. A. Atwater and A. Polman, *Nature Mater.* **9**, 205 (2010).
- ⁵P. Spinelli, M. Hebbink, R. de Waele, L. Black, F. Lenzmann, and A. Polman, *Nano Lett.* **11**, 1760 (2011).
- ⁶M. A. Green and S. Pillai, *Nat. Photonics* **6**, 130 (2012).
- ⁷S. H. Lim, W. Mar, P. Matheu, D. Derkacs, and E. T. Yu, *J. Appl. Phys.* **101**, 104309 (2007).
- ⁸D. Derkacs, S. H. Lim, P. Matheu, W. Mar, and E. T. Yu, *Appl. Phys. Lett.* **89**, 093103 (2006).
- ⁹S. Pillai, K. R. Catchpole, T. Trupke, and M. A. Green, *J. Appl. Phys.* **101**, 093105 (2007).
- ¹⁰Y. Zhang, Z. Ouyang, N. Stokes, B. Jia, Z. Shi, and M. Gu, *Appl. Phys. Lett.* **100**, 151101 (2012).
- ¹¹Y. N. Zhang, X. Chen, Z. Ouyang, H. Y. Lu, B. H. Jia, Z. R. Shi, and M. Gu, *Opt. Mater. Express* **3**, 489 (2013).
- ¹²K. Nakayama, K. Tanabe, and H. A. Atwater, *Appl. Phys. Lett.* **93**, 121904 (2008).
- ¹³S. Mokkaapati, F. J. Beck, R. de Waele, A. Polman, and K. R. Catchpole, *J. Phys. D: Appl. Phys.* **44**, 185101 (2011).
- ¹⁴T. Xu, M. G. Kang, H. J. Park, and L. J. Guo, *Proc. SPIE* **7933**, 793329 (2011).
- ¹⁵J. Mertz, *J. Opt. Soc. Am. B* **17**, 1906 (2000).
- ¹⁶C. C. Chao, C. M. Wang, Y. C. Chang, and J. Y. Chang, *Opt. Rev.* **16**, 343 (2009).
- ¹⁷Z. Ouyang, X. Zhao, S. Varlamov, Y. G. Tao, J. Wong, and S. Pillai, *Prog. Photovoltaics* **19**, 917 (2011).
- ¹⁸P. Spinelli, V. E. Ferry, J. van de Groep, M. van Lare, M. A. Verschuuren, R. E. I. Schropp, H. A. Atwater, and A. Polman, *J. Opt.* **14**, 024002 (2012).
- ¹⁹Z. J. Sun, X. L. Zuo, and Y. Yang, *Opt. Lett.* **37**, 641 (2012).
- ²⁰D. M. Schaadt, B. Feng, and E. T. Yu, *Appl. Phys. Lett.* **86**, 063106 (2005).
- ²¹S. Fahr, C. Rockstuhl, and F. Lederer, *Appl. Phys. Lett.* **97**, 173510 (2010).
- ²²P. Y. Silvert, R. Herrera Urbina, N. Duvauchelle, V. Vijaykrishnan, and K. T. Elhsissen, *J. Mater. Chem.* **6**, 573 (1996).
- ²³Lumerical Solutions Inc., Vancouver, British Columbia, Canada (Accredited in June 2013).